Control and Design of Engineering Mechanics Systems

Esubalewe Lakie Yedeg

Licentiate Thesis, May 2013

Department of Computing Science
Umeå University
SE-901 87 Umeå
Sweden

List of Papers

This thesis consists of an introduction to optimal control and topology optimization problems and the following two papers:

Paper A Esubalewe Lakie Yedeg and Eddie Wadbro. Optimal ball pitching. In review for *Mechanism and Machine Theory*.

Paper B Esubalewe Lakie Yedeg, Eddie Wadbro, and Martin Berggren. Anisotropic Topology Optimization of a Reactive Muffler with a Perforated Pipe. Submitted for publication.

Acknowledgement

First of all, I would like to express my deepest respect and most sincere gratitude to my supervisors Prof. Martin Berggren and Dr. Eddie Wadbro, for offering me the opportunity to carry out my PhD study in the Department of Computing Science, for their continuous guidance, invaluable discussion, understanding, and encouragement. Their constructive criticism and excellent advice in this work are highly appreciated.

My deep gratitude also goes to my colleagues and friends for their assistance and giving me a pleasant working atmosphere.

A very special appreciation goes to my wife Tigist Muluken for her unreserved love, understanding and encouragement. I thank her for being on my side far away from her parents and giving me a constant support. Finally, I would like to thank my parents and friends in Ethiopia for their support and motivation.

Contents

Chapter 1

Introduction

Many mechanical systems can be modeled by mathematical relations such as ordinary differential equations. These systems change with respect to time or any other independent variable according to the relation. It is often possible to guide these systems from one state to another predefined state by applying some kind of external force or control. It may also be possible to carry out the same task in different ways. If there are more than one way of performing the task, then it may be possible to choose the "best" way. The best way can be quantified using a measure of performance of the system; this measure is often called "cost function", "objective function", or "performance index". The external force applied to the system corresponding to the best performance is called the "optimal" control.

Optimal control also denotes the process of determining control and state trajectories for a system over a given period of time to minimize or maximize an objective function. Optimal control is related to the theory of calculus of variations. The theory of optimal control has been widely studied and is used in many areas since the beginning of the so-called "modern" control theory in the 1960s.

In general, control systems are classified into two broad categories: *closed loop* and *open loop* systems. In closed-loop systems, also called *feedback* control systems, the input is affected by the systems output directly or indirectly. It uses the input and some portion of the output to maintain a prescribed relationship between the output and the reference input. However, in open-loop control systems, sometimes called *off-line* or *non-feedback* control systems, the system output does not affect the control input in any form. In this case, the system is free from any change in response to the output of the process. Standard control theory mostly concerns closed-loop systems, and these are the ones used in most engineering control applications. In contrast, the open-loop systems are useful in more special situations. In this thesis, we consider the design of such an open-loop system.

Many mechanical devices play an important role in our daily life. How to "optimally" design them while satisfying the required system and design constraints is an important engineering concern. The systems can often be modeled by partial differential equations, such as the equations of elasticity, fluid mechanics, or acoustics.

The optimality of the design can be measured by using an objective function that evaluates for example construction cost, strength of the designed structure, or some other performance measure. If a particular design makes the objective function as high or low as possible, depending the objective, it is called an optimal design.

Design optimization of mechanical devices seeks to acquire the best performance of the structure while satisfying some kind of constraints. Optimal design is becoming more important due to resource material limitations, the development of computational algorithms, and the availability of high-speed computers. In the last three decades the subject has developed rapidly with new theoretical insights, computational methods, and application areas. Design optimizations in general can be classified into three main groups, namely, *sizing optimization*, *shape optimization*, and *topology optimization*.

In sizing optimization, the conceptual geometry of the design is fixed during the optimization process, and the goal is to find the optimal values of some free parameters of the structure, such as thickness, length, radius, etcetera. In shape optimization problems, the shape of the boundaries is subject to optimization but the conceptual design is still predetermined. The design variables are some kind of parameterization of the design boundaries. Topology optimization is the most general and flexible approach in structural optimization, where for every point in the design region, it is to be determined whether the point is occupied by a material or not. Thus, the topology of the structure is not known a priori. Topology optimization can be seen as a generalization of sizing and shape optimization.

In this thesis, we use the optimal control and topology optimization ideas in two different areas. First we apply the optimal control approach to determine the control of a ball pitching robot in order to throw a ball as far as possible. The open-loop control problem is solved numerically by using Matlab's `fmincon`. Then the topology optimization method is used to determine the internal layout of a reactive muffler in order to minimize the acoustic energy at the outlet. The Method of Moving Asymptotes is used to solve the optimization problem.

The rest of this comprehensive summary is organized as follows. In Chapter 2, a brief introduction to optimal control theory is presented. It is followed by the summary of Paper A in Chapter 3. Then a short introduction to topology optimization by material distribution is included in Chapter 4. Finally Chapter 5 presents the summary of Paper B.

Chapter 2

Optimal Control

The subject of optimal control addresses the problem of finding a control input for a given system that optimizes a certain measure, or performance criterion. Optimal control has been under development for many years, and the subject is widely used in many application areas. Several surveys on the development of optimal control theory can be found in the literature. Bryson [1] presents the history of optimal control from 1950 to 1985 including the history of calculus of variations since the 1600s. A brief historical survey of the development of the calculus of variations and optimal control is presents by Sargent [2]. He also reviews different approaches to the numerical solution of optimal control problems. Betts [3] reviews numerical methods for trajectory optimization problems. There are several books on the theory of optimal control (for instance Bryson and Ho [4], Hestenes [5], Bryson [6], and Hull [7]). The next sections contain a brief introduction to open-loop optimal control problems.

2.1 Formulation of an optimal control problem

A simplified version of the optimal control problem presented in Paper A can be formulated as follows. Given a final time t_f, find a control $u(t) \in \mathbb{R}^m$ that minimizes the objective function

$$J(u) = \phi(x(t_f), t_f) \tag{2.1}$$

subject to differential equation

$$\begin{aligned} \dot{x}(t) &= f(x(t), u(t), t), \quad t_0 \leq t \leq t_f, \\ x(t_0) &= x_0, \end{aligned} \tag{2.2}$$

constraints on the control and state variables

$$c(x(t), u(t), t) \leq 0, \quad t_0 \leq t \leq t_f, \tag{2.3}$$

and terminal condition

$$\psi(x(t_f), t_f) = 0. \tag{2.4}$$

Here, the control and state variables are denoted by $u(t) = (u_1(t), \ldots, u_m(t))^T$ and $x(t) = (x_1(t), \ldots, x_n(t))^T$, respectively. The functions $\phi : \mathbb{R}^{n+1} \to \mathbb{R}$, $f : \mathbb{R}^{n+m+1} \to \mathbb{R}^n$, $c : \mathbb{R}^{n+m+1} \to \mathbb{R}^l$, and $\psi : \mathbb{R}^{n+1} \to \mathbb{R}$ are continuously differentiable.

The system of first-order ordinary differential equations (2.2) describes the dynamics of the system. In control theory, this is called the state-space representation of the system dynamics. Sometimes, the dynamics of the system may depend on higher order derivatives of the state variable. It is usually convenient to rewrite such systems to the state-space form (2.2). An optimal control problem of the above form is known as a *Mayer problem*.

Remark: A problem with integral cost $\int_{t_0}^{t_f} L((x(t), u(t), t)\, dt$ can be formulated in Mayer form by introducing an additional state variable x_L following the dynamics

$$\dot{x}_L = L((x(t), u(t), t), \quad t_0 \leq t \leq t_f, \quad \text{with } x_L(t_0) = 0.$$

2.2 Numerical Methods

For some optimal control problems, it is possible to obtain analytical solutions from the necessary and sufficient optimality conditions [8, 9, 10]. However, optimal control problems are typically non-linear and do not possess analytical solutions in most cases. Hence, it is in general necessary to employ numerical methods to solve optimal control problems. Numerical methods for optimal control problems are generally classified into *indirect methods* and *direct methods* [3, 11].

2.2.1 Indirect methods

In indirect methods, the calculus of variations or Pontryagin's maximum principle [4, 5, 8] are employed to formulate the first-order optimality conditions of the optimal control problem (2.1) – (2.4). These methods transform the original optimal control problem into a boundary-value problem, which can be solved using standard techniques for differential equations. *First-order necessary conditions of optimality* can be obtained by applying calculus of variations to the optimal control problem. These conditions are usually derived by using the so-called *Hamiltonian function*

$$H(x, \lambda, \mu, u, t) = \lambda^T(t) f(x, u, t) + \mu^T(t) c(x, u, t), \tag{2.5}$$

and the *auxiliary function*

$$\Phi(x(t_f), t_f) = \phi(x, t_f) + \nu^T(t_f) \psi(x, t_f), \tag{2.6}$$

where $\lambda(t) \in \mathbb{R}^n$ is the *costate* or *adjoint variable* and $\mu(t) \in \mathbb{R}^l$ is a Lagrangian multiplier associated with the constraint (2.3). The existence of λ and μ is discussed in the books by Pontryagin [8], Bryson and Ho [4], and Kirk [10]. The first-order optimality conditions of the problem (2.1) – (2.4) are given by

$$\dot{\lambda} = -\frac{\partial H}{\partial x} = -\lambda^T \frac{\partial f}{\partial x} - \mu^T \frac{\partial c}{\partial x}, \tag{2.7}$$

$$0 = \frac{\partial H}{\partial u} = \lambda^T \frac{\partial f}{\partial u} + \mu^T \frac{\partial c}{\partial u}, \tag{2.8}$$

and

$$\lambda(t_f) = \frac{\partial \Phi}{\partial x}|_{t=t_f}, \quad (\frac{\partial \Phi}{\partial t} + H)|_{t=t_f} = 0, \tag{2.9}$$

in addition to state equation (2.2), constraint (2.3), terminal condition (2.4), and the *complementary slackness conditions*

$$\mu_i c_i = 0, \quad i = 1 \dots l. \tag{2.10}$$

The differential equation (2.7) is usually called *costate* or *adjoint equation* and the equations in (2.9) are called *transversality conditions*. A detailed derivation of equations (2.7)–(2.10) can be found in books by Bryson [4] and Kirk [10].

Numerical methods for general boundary-value problems can be used to obtain the solutions of these necessary conditions. The three most common methods are the *shooting method*, the *multiple-shooting method* and the *collocation method*. A detailed description of these methods can be found in articles by Betts [3], Rao [12], Stryk and Bulirsch [11], and the references therein.

2.2.2 Direct methods

In direct methods, the original continuous optimal control problem is transcribed to a non-linear programming problem. This is based on a parametrization of the control and/or the state variables in some appropriate manner. There are different methods to transcribe optimal control problem (2.1) – (2.4) into a non-linear programming problem (NLP), for instance, direct (multiple) shooting methods in which only the control variable is parameterized, and direct collocation method, which is a state and control parametrization method [3, 12, 13, 14]. In these methods, the control and/or state variables become parameter dependent and the optimization is carried out with respect to the parameters. The resulting parameter optimization problem can be solved using one of the several available non-linear programming algorithms.

It is also possible to transform the continuous optimal control problem into its discrete equivalence. In our work we approximate the control variable by a piecewise constant function and the state variable is approximated at a finite number of discrete time points. The state equation (2.2) is solved by using a numerical method for differential equations, and the path constraint (2.3) is transcribed into finite number of vector constraints. The discretization is presented in the following section.

2.3 Discretization

In this section we use a discretization method to transform the infinite dimensional optimal control problem (2.1) – (2.4) into a finite dimensional non-linear optimization problem. There are various numerical methods that can solve differential equation (2.2), for instance, *Euler methods*, *Adams-Bashforth* and *Adams-Moulton multiple-step methods*, and *Runge-Kutta methods*, to list a few [12, 15, 16]. We use the so-called *Heun's method* to solve state equation (2.2) numerically. Thus, the total time interval $[t_0, t_f]$ is divided into N equal subinterval of length $\Delta t = (t_f - t_0)/N$ each. The subintervals are denoted by $[t_{k-1}, t_k]$, for $k = 1, \ldots, N$, where the *node* points are defined by

$$t_k = t_0 + k\Delta t, \quad k = 1, \ldots, N, \tag{2.11}$$

with $t_N = t_f$.

We approximate the control function u by a piecewise constant function u_d, defined by

$$u_d(t) = u^k \text{ for } t_{k-1} \leq t \leq t_k, \quad k = 1, \ldots, N, \tag{2.12}$$

and let x^k denote the approximation of the state variable $x(t)$ at time $t = t_k$. Then starting from $x^0 = x(t_0)$, the subsequent states $x^k, k = 1, \ldots, N$ are computed according to

$$\tilde{x}^k = x^{k-1} + \Delta t f(x^{k-1}, u^k, t_{k-1}), \tag{2.13a}$$

$$x^k = x^{k-1} + \frac{\Delta t}{2}\big(f(x^{k-1}, u^k, t_{k-1}) + f(\tilde{x}^k, u^k, t_k)\big). \tag{2.13b}$$

This approach gives the discrete state equation

$$\mathbf{0} = \mathbf{F}(\mathbf{x}, \mathbf{u}, \mathbf{t}) = \begin{pmatrix} F_1(x^0, x^1, u^1, t_0, t_1) \\ \vdots \\ F_N(x^{N-1}, x^N, u^N, t_{N-1}, t_N) \end{pmatrix}, \tag{2.14}$$

where $\mathbf{x} = (x^1, \ldots, x^N)$, $\mathbf{u} = (u^1, \ldots, u^N)$, $\mathbf{t} = (t_1, \ldots, t_N)$, and

$$F_k(x^{k-1}, x^k, u^k, t_{k-1}, t_k) = x^{k-1} + \frac{\Delta t}{2}\big(f(x^{k-1}, u^k, t_{k-1}) + f(\tilde{x}^{k-1}, u^k, t_k)\big) - x^k$$

with $\tilde{x}^k$ defined in expression (2.13a), for $k = 1, \ldots, N$.

Remark: In Paper A we use a slightly different version of the time discretization in order to allow the final time t_f to change.

The constraints on the control and the state variables (2.3) can be imposed on the discrete control and state variables. This can be done by evaluating the constraints at the node points. Thus the discrete constraints become

$$c(x^k, u^k, t_k) \leq 0, \quad k = 1, \ldots, N. \tag{2.15}$$

Similarly, the discrete objective function and the terminal condition are obtained by replacing the state variable and the time at $t = t_f$ by their discrete values

$$\tilde{J}(\mathbf{u}) = \phi(x^N, t_N),$$

and

$$\psi(x^N, t_N) = 0.$$

Thus the continuous optimal control problem (2.1)–(2.4) is transformed into the following discrete formulation

$$\begin{aligned} \min_{\mathbf{u}} \ & \tilde{J}(\mathbf{u}) \\ \text{subject to } & \mathbf{F}(\mathbf{x}, \mathbf{u}, \mathbf{t}) = 0, \\ & c(x^k, u^k, t_k) \leq 0, \quad k = 1, \ldots, N, \\ & \psi(x^N, t_N) = 0, \\ & x^0 = x_0. \end{aligned} \tag{2.16}$$

The discrete optimal control problem (2.16) can be solved by gradient-based algorithms. Gradient-based algorithms are widely used and are regarded as the most reliable methods for optimal control problems with state constraints [1, 17]. There are many variants of gradient-based algorithms with different properties. In Paper A, we use an interior point method as implemented in Matlab's `fmincon`. The algorithm needs the first-order derivatives of the objective function and the constraint functions. We use the discrete adjoint equations to calculate the gradients.

2.4 Discrete adjoint based gradient computation

In the discrete adjoint based gradient computation approach, we solve the discrete state equation forward in time and then the discrete adjoint problem backward in time. To compute the gradient of the objective function with respect to the control variable $\mathbf{u}$, let $\mathbf{x}$ be the solution of the discrete state equation

$$\mathbf{F}(\mathbf{x}, \mathbf{u}, \mathbf{t}) = 0. \tag{2.17}$$

The gradient of the objective function with respect to $\mathbf{u}$, using the chain rule can be written as

$$\nabla_{\mathbf{u}} \tilde{J} = \frac{\partial \phi}{\partial \mathbf{x}} \frac{d\mathbf{x}}{d\mathbf{u}} \tag{2.18}$$

with ϕ defined in expression (2.1). The $d\mathbf{x}/d\mathbf{u}$ term can be determined from the derivative of the state equation (2.17). Differentiation of state equation (2.17) with respect to $\mathbf{u}$ yields

$$\left(\frac{\partial \mathbf{F}}{\partial \mathbf{x}}\right) \frac{d\mathbf{x}}{d\mathbf{u}} + \frac{\partial \mathbf{F}}{\partial \mathbf{u}} = 0. \tag{2.19}$$

Let $\boldsymbol{\lambda}$ be the solution of the adjoint equation

$$\boldsymbol{\lambda}^T \frac{\partial \mathbf{F}}{\partial \mathbf{x}} = \frac{\partial \phi}{\partial \mathbf{x}}. \tag{2.20}$$

Multiplying both sides of equation (2.19) by $\boldsymbol{\lambda}^T$ yields

$$\left(\boldsymbol{\lambda}^T \frac{\partial \mathbf{F}}{\partial \mathbf{x}}\right) \frac{d\mathbf{x}}{d\mathbf{u}} + \boldsymbol{\lambda}^T \frac{\partial \mathbf{F}}{\partial \mathbf{u}} = 0. \tag{2.21}$$

By combining equations (2.20) and (2.21) we obtain

$$\frac{\partial \phi}{\partial \mathbf{x}} \frac{d\mathbf{x}}{d\mathbf{u}} + \boldsymbol{\lambda}^T \frac{\partial \mathbf{F}}{\partial \mathbf{u}} = 0. \tag{2.22}$$

Finally, by comparing equation (2.18) and equation (2.22), we obtain the gradient of the objective function in terms the of the adjoint variable

$$\nabla_{\mathbf{u}} \tilde{J} = -\boldsymbol{\lambda}^T \frac{\partial \mathbf{F}}{\partial \mathbf{u}}. \tag{2.23}$$

Following the same procedure as above, for each $i = 1, \ldots, l$ the gradient of the constraint function c_i is obtained by

$$\nabla_{\mathbf{u}} c_i = \frac{\partial c_i}{\partial \mathbf{u}} - \boldsymbol{\mu}_i^T \frac{\partial \mathbf{F}}{\partial \mathbf{u}}, \tag{2.24}$$

where $\boldsymbol{\mu}_i$ is the solution of

$$\boldsymbol{\mu}_{\boldsymbol{i}}^T \left(\frac{\partial \mathbf{F}}{\partial \mathbf{x}}\right) = \frac{\partial c_i}{\partial \mathbf{x}}. \tag{2.25}$$

Chapter 3

Summary of Paper A - Optimal Ball Pitching

3.1 Introduction

In Paper A, we study an optimal control problem of a ball pitching robot that is designed to capture important dynamics of the human upper limb (including the shoulder, arm, and forearm) during an overarm throw. The robot has two links that are connected at the *elbow* joint by a linear torsional spring. The links represent the arm and forearm, and the spring represents the stiffness of the muscles around the elbow joint in human upper limb [18, 19]. The two-link robot is connected to a motor shaft at the *shoulder* joint by a non-linear torsional spring. At the end of the forearm, the robot is equipped with a gripping mechanism that allows the robot to grasp and release the ball at any required time.

The main objective is to determine the optimal motor torque and the release time that enable the robot to pitch the ball as far as possible. We include constraints on the motor torque and power as well as the angular velocity of the motor shaft into the problem formulation. For computational efficiency, we replace the time-global constraints on maximum allowed power and maximum angular velocity of the motor shaft by approximations based on integral quantities.

3.2 Problem formulation

The initial configuration of the two-link robot with a gripping mechanism holding a ball is illustrated in Figure 3.1. We denote the two links by the *arm* and *forearm*, respectively. Let q_2 measure the angle change between the arm and the forearm at the elbow joint. The angles q_1 and q_m, measured with respect to the horizontal axis, describe the configuration of the arm and the motor shaft, respectively. The only driving force of the system comes from the motor shaft. Figure 3.2 shows a trajectory of the ball during a pitching motion. The ball gets released with velocity v_b in the

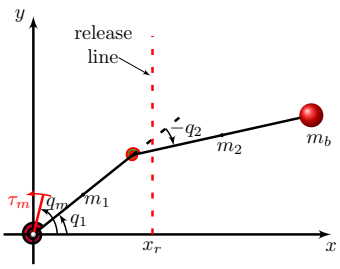

Figure 3.1: Initial configuration of the pitching robot and the release line.

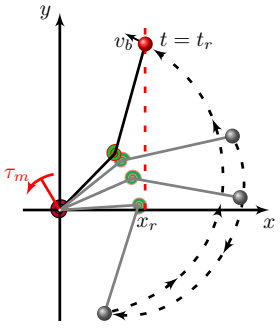

Figure 3.2: Configuration of the pitching robot at the release time and the ball trajectory during the pitching motion.

desired direction when it crosses the release line, $(x, y) = (x_r, s), s \in \mathbb{R}$.

Let $q = [q_m, q_1, q_2]^T$ be a vector of generalized coordinates of the robotic manipulator, and let $\theta(t) = [q(t), \dot{q}(t)]^T \in \mathbb{R}^6$ be the state vector. Let $\tau(t) \in \mathbb{R}$ be a variable that measures the torque of the motor. The equations of motion of the system, derived based on the Euler–Lagrange formulation in Appendix A of Paper A, in state space representation becomes

$$\dot{\theta} = f(\theta, \tau), \tag{3.1}$$

where,

$$f(\theta, \tau) = \begin{bmatrix} \theta_4 \\ \theta_5 \\ \theta_6 \\ I_m^{-1}(\tau - \tau_s(\theta)) \\ M(\theta)^{-1}\left(K(\theta) - G(\theta) - C(\theta)\begin{bmatrix}\theta_4 \\ \theta_5\end{bmatrix}\right) \end{bmatrix}, \tag{3.2}$$

and where, I_m is the motor inertia, $\tau_s(\theta)$ the torque due to the non-linear spring at the shoulder joint, $M(\theta)$ the inertia matrix, $C(\theta)$ the matrix of centrifugal and Coriolis forces, and the vectors $G(\theta)$ and $K(\theta)$ represent gravitational and spring forces, respectively.

As illustrated in Figure 3.2, at time $t = t_r$ the ball is released with velocity v_b. It then follows a ballistic trajectory until it hits the ground at a point $(J, 0)$, where

$$J(\theta, x_r) = x_r + \frac{\dot{x}_b(t_r)}{g}\left(\dot{y}_b(t_r) + \sqrt{\dot{y}_b(t_r)^2 + 2g y_b(t_r)}\right). \tag{3.3}$$

Here x_r is the position of the vertical release line, $(x, y) = (x_r, s)$, $s \in \mathbb{R}$, at which the gripping mechanism of the robot releases the ball, and g is the gravitational constant. The vertical position of the ball at the release time is

$$y_b(t_r) = l_1 \sin(q_1(t_r)) + l_2 \sin(q_1(t_r) + q_2(t_r)),$$

where l_1 and l_2 are the lengths of the arm and the forearm, respectively. Similarly, the velocity of the ball $v_b = (\dot{x}_b, \dot{y}_b)$ at time $t = r_r$ is given by

$$\begin{aligned}\dot{x}_b(t_r) &= -l_1 \sin(q_1(t_r))\dot{q}_1(t_r) - l_2 \sin(q_1(t_r) + q_2(t_r))(\dot{q}_1(t_r) + \dot{q}_2(t_r)),\\ \dot{y}_b(t_r) &= l_1 \cos(q_1(t_r))\dot{q}_1(t_r) + l_2 \cos(q_1(t_r) + q_2(t_r))(\dot{q}_1(t_r) + \dot{q}_2(t_r)).\end{aligned}$$

Note that the robot's shoulder is held fixed at the origin of the coordinate system and that the ball has thrown in the negative x direction. Hence, minimizing J implies maximizing the distance between the origin and the point $(J, 0)$.

We minimize J over the torque change in time. By inclusion of the constraints on the motor torque and torque change in the set of admissible controls we obtain

$$\mathcal{A} = \left\{ \eta \in L^\infty \mid \sup_t |\eta(t)| \leq C_\tau, \ \sup_t \left| \tau_0 + \int_0^t \eta(s)\,\mathrm{d}s \right| \leq \bar{\tau} \right\}, \tag{3.4}$$

where $\bar{\tau}$ is the maximum allowed torque of the motor, C_τ is the bound on the torque change in time, and η is the our control function defined by

$$\begin{aligned}\dot{\tau} &= \eta,\\ \tau(0) &= \tau_0.\end{aligned} \tag{3.5}$$

For computational efficiency, we replace the time-global constraints on maximum allowed power and maximum angular velocity of the motor shaft by approximations based on integral quantities (see Paper A for the discussion). For practical reasons, we impose the constraint $|x_r| \leq L$ on the release line, where $L = l_1 + l_2$. Since it is possible to determine the release line position if the release time is known and vice versa, we optimize with respect to the release line position instead of the time.

Putting the system dynamics, the objective function, and the constraints together, we obtain the optimal control problem

$$\begin{aligned}\min_{\substack{\eta\in\mathcal{A},\\ |x_r|\leq L}} \quad & J(x_r, \theta(t_r))\\ \text{subject to} \quad & \dot{\tau} = \eta, \ \ \tau(0) = \tau_0,\\ & \dot{\theta} = f(\theta, \tau), \ \ \theta(0) = \theta^{(0)},\\ & \left(\frac{1}{t_r}\int_0^{t_r} |\theta_4|^p \,\mathrm{d}t\right)^{1/p} \leq \left(\frac{1}{p+1}\right)^{1/p} Q_{\max},\\ & \left(\frac{1}{t_r}\int_0^{t_r} |\tau\theta_4|^p \,\mathrm{d}t\right)^{1/p} \leq \left(\frac{1}{p+1}\right)^{1/p} P_{\max},\end{aligned} \tag{3.6}$$

where $Q_{\max}$ and $P_{\max}$ are the maximum allowed angular velocity of the motor shaft and input power of the motor, respectively, and $\theta^{(0)}$ is the initial state of the system.

We discretize the optimal control problem (3.6) using the strategies discussed in Section 2.3. The discrete version of optimal control problem (3.6) is solved numerically using an interior point method with BFGS Hessian approximation as implemented in Matlab's `fmincon`. The gradients of the objective function and the constraint function is computed by using the discrete adjoint approach.

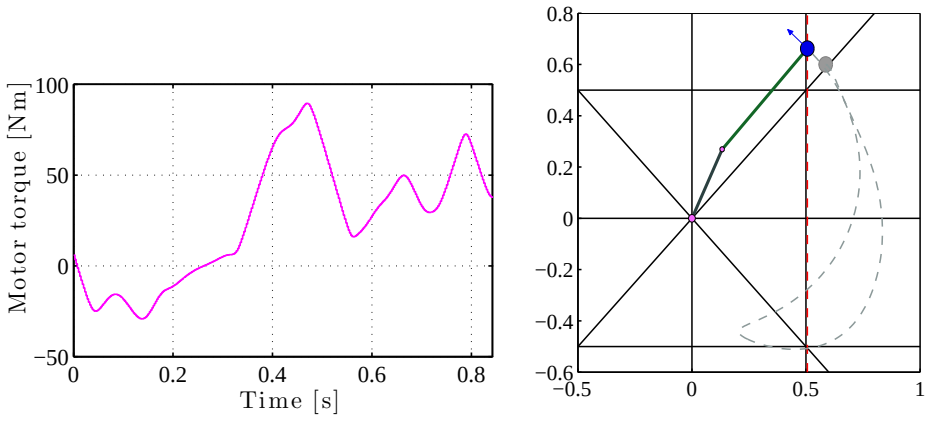

Figure 3.3: Left: the time evaluation of the optimal torque; Right: the ball trajectory during the pitching motion, starting from the initial position up to the time when the ball is released.

3.3 Selected numerical results

We use with interior point and BFGS Hessian approximation options to solve the optimal control problem numerically. The non-linear spring at the shoulder joint produces a torque, that is approximated by the function

$$\tau_s = 7761.7(q_m - q_1)^3 + 2.9755(q_m - q_1)^2 + 77.8080(q_m - q_1) - 0.0334.$$

The coefficients are obtained from a least-squares fit with measured data, for the pitching robot we study, in the range $|q_m - q_1| \leq 0.25$ rad. In this range, the relative error between the measured data and the cubic model is less than 2.5×10^{-3}.

The initial conditions on the generalized coordinates

$$q_0 = [0.908, -0.172, 0.978] \text{ rad}, \quad \dot{q}_0 = 0 \text{ rad/s},$$

and the motor torque $\tau_0 = 8.213$ Nm are determined in such away that the system is stationary at time $t_0 = 0$ for a given $q_1(0) = \pi - 2.234$ rad. We impose the following natural constraint on the release line position

$$|x_r| \leq l_1 + l_2,$$

where $l_1 = 0.3$ m and $l_1 = 0.542$ m are the lengths of the arm and the forearm, respectively. The maximum allowed motor torque, power and angular velocity of the motor shaft are $\bar{\tau} = 180$ Nm, $P_{\max} = 270$ Nm/s and $Q_{\max} = 3.787$ rad/s, respectively. Refer to Paper A for a complete set of parameters for this experiment. We set $T = 2$ s, $\Delta t = 0.0025$ s, $C_\tau = 1000$ Nm/s, and $p = 100$ for the numerical experiments.

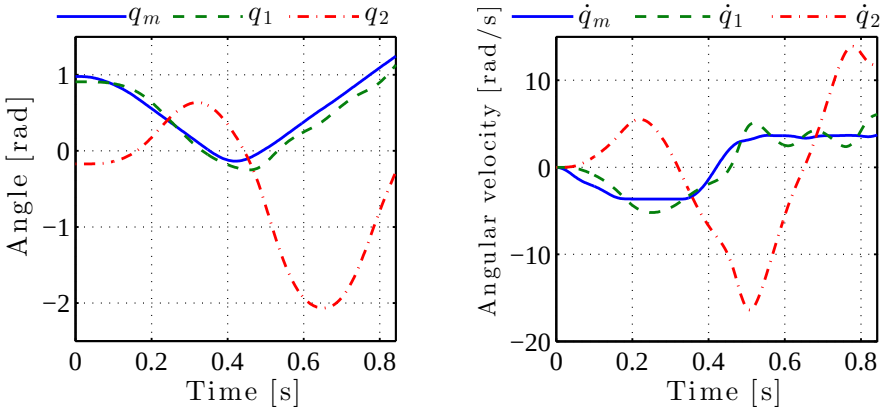

Figure 3.4: Time evolution of the generalized coordinates q_1, q_2, and q_m (left), the corresponding angular velocities $\dot{q}_1, \dot{q}_2$ and $\dot{q}_m$ (right) computed using the optimal input torque from Figure 3.3.

Figure 3.3 shows the time evaluation of the resulting optimal input torque profile (left diagram) and the ball trajectory during the pitching motion (right diagram). The torque profile shows that the optimal torque attains its maximum value 89.54 Nm after 0.473 s. The optimal release line given by $(x, y) = (x_r, s)$, where $x_r = 0.506$ m and $s \in \mathbb{R}$, and the pitching motion takes $t_r = 0.843$ s to cross the release line. The ball is thrown at an upward angle of 40.82 degrees with velocity of 11.36 m/s. After the ball is released, it follows a ballistic trajectory in the negative direction and finally hits the ground 13.25 m away from the origin (the robot's shoulder position).

Figure 3.4 illustrates the time evolution, from the initial time to the final time, of the generalized coordinates q_1, q_2, and q_m (left diagram), and the angular velocities $\dot{q}_1, \dot{q}_2$ and $\dot{q}_m$ (right diagram). Note that q_2 measures the angle change between the arm and the forearm, while q_1 and q_m measure the angle of the arm and the motor shaft with respect to the horizontal line. The left diagram illustrates, in particular, that $|q_m - q_1| \leq 0.25$ rad throughout the motion.

From the right diagram of Figure 3.4, we can see that the angular velocity $\dot{q}_m$ of the motor shaft (solid line) essentially has four phases. Starting from a stationary position, in the first phase it decelerates from a stationary position until it reaches an angular velocity of about -3.7 rad/s. The motor shaft moves at an almost constant angular velocity in the second phase, and it is followed by a fast acceleration in the third phase. Finally, the motor shaft moves at a relatively constant angular velocity of about 3.7 rad/s. In the second and last phase the angular speed $\dot{q}_m$ of the motor shaft reached to the maximum bound. During the last phase, the angular velocity, $\dot{q}_1 + \dot{q}_2$ of the forearm measured with respect to the horizontal line is strictly increasing during the last 0.35 s of the pitching motion. This rapid increment accelerates the ball very fast as time close to releasing, and it maximizes the distance thrown.

Chapter 4

Topology Optimization by Material Distribution

Topology optimization is a mathematical approach that optimizes the material layout of a device within a given design space such that a certain performance criterion is maximized or minimized for a given set of conditions. Starting from the publication of the pioneering paper by Bendsøe and Kikuchi [20], topology optimization methods for continuum structures have been expanded significantly and applied to many practical engineering problems. Topology optimization has been used starting from designing materials at micro-level (example Sigmund [21], Zhou and Li [22], and Jensen et al. [23]) to large-scale designs such as bridges and buildings, and for components within the automobile and aircraft industries (example Borrvall and Petersson [24], Guan et al. [25], Wang et al. [26], and Krog et al. [27]). The area of topology optimization is dominated by methods that apply the *material distribution* concept. Most numerical methods for topology optimization are based on finite element methods. In this case, the design domain is discretized into a fine mesh of elements, and the purpose of the algorithm is to find the optimal material distribution by determining for each element in the design domain whether it should be filled with material (solid element) or not (element with air). In the next sections, a brief overview on topology optimization by the material distribution method is introduced.

4.1 Problem formulation

In general, a topology optimization problem consists of an objective function, a design domain, a design constraint, and a state equation. Let Ω be the design domain and $\Omega_{\mathrm{m}} \subset \Omega$ the region in the design domain occupied by solid material. The distribution of material in Ω is usually modeled by using a material indicator function α, defined as $\alpha(x) = 1$, if $x \in \Omega_{\mathrm{m}}$ and $\alpha(x) = 0$ otherwise. Mathematically, a topology optimization

problem in its general form is given by

$$\min_{\alpha \in U} J(\alpha, u) \tag{4.1a}$$

$$\text{s.t. } a(\alpha; u, v) = \ell(v), \quad \forall v \in \mathcal{V}, \tag{4.1b}$$

$$C(\alpha, u) \leq 0, \tag{4.1c}$$

where $U = \{\alpha : \alpha(x) \in \{0, 1\}, x \in \Omega\}$ is the set of admissible designs, J is an objective function to measure the performance, u denotes the state variable, C is a constraint function, and $\mathcal{V}$ is an appropriate functional space. The design and the state variables are related by the state equation, in this case given by the variational form (4.1b).

Remark: In acoustic related topology optimization problems the material indicator function α is 1 in region of air and 0 in the region which is occupied by sound-hard material.

The prototype problem of this kind is the classical problem of minimizing the compliance, $J = \ell(u)$ (equivalent to maximizing the stiffness), of a mechanical structure subject to state equation (4.1b), the governing equation of linear elasticity, and the volume constraint, $C(\alpha) = \int_\Omega \alpha(x)dx - V \leq 0$. Here, V is the upper bound of the volume occupied by solid material. In order to guarantee coercivity of the bilinear form, the material indicator function should not be zero. Therefore, the space of admissible designs $U = \{\alpha : \alpha(x) \in \{0, 1\}, x \in \Omega\}$ is usually replaced by $U = \{\alpha : \alpha(x) \in \{\varepsilon, 1\}, x \in \Omega\}$ for a small constant $\varepsilon > 0$, such that $\alpha(x) = \varepsilon$ for $x \in \Omega - \Omega_{\mathrm{m}}$.

In many cases, topology optimization problems of the form (4.1) are ill-posed. Typically, the ill-posedness is due to the existence of a sequence of minimizers that do not converge [28], which, after discretization, manifests itself as mesh dependency in the numerical solution. A relaxation method can be used to address this problem. It also allows the use of gradient-based optimization algorithms. By letting α take values in the continuous range $[\varepsilon, 1]$, the binary optimization problem (4.1) becomes

$$\min_{\alpha \in \mathcal{U}} J(\alpha, u), \tag{4.2a}$$

$$\text{s.t. } a(\alpha; u, v) = \ell(v), \quad \forall v \in \mathcal{V}, \tag{4.2b}$$

$$C(\alpha, u) \leq 0, \tag{4.2c}$$

where $\mathcal{U} = \{\alpha : \varepsilon \leq \alpha(x) \leq 1, x \in \Omega\}$.

In the case of compliance minimization, there exist a unique solution of problem (4.2). The proof of the existence of a solution can be found in Section 5.2 of the book [29] by Bendsøe and Sigmund.

4.2 Discretization

Numerical methods are typically used to obtain an approximate solution of optimization problem (4.2). Following a finite element procedure, the domain Ω is partitioned

into N small subdomains called elements $E_k, k = 1, \ldots, N$, such that $\overline{\Omega} = \cup_{k=1}^{N} \overline{E}_k$. The material indicator function α is approximated by α_h, an element-wise constant function. The state variable u is approximated by $u_h \in \mathcal{V}^h(\Omega)$, where $\mathcal{V}^h \subset \mathcal{V}$ is the space of continuous and element-wise polynomial functions. The discrete state variable u_h is the solution of the discrete state equation for a given feasible design α_h

$$a_h(\alpha_h; u_h, v_h) = \ell_h(v_h), \quad \forall v_h \in \mathcal{V}^h, \tag{4.3}$$

where v_h, a_h and ℓ_h are the discretized version of v, a and ℓ, respectively. Similarly, the objective and constraint functions are replaced by their corresponding discrete version.

Then the discrete version of the optimization problem (4.2) can be formulated as

$$\begin{aligned} \min_{\alpha_h \in \mathcal{U}_h} \; & J_h(\alpha_h, u_h) \\ \text{s.t. } & a_h(\alpha_h; u_h, v_h) = \ell_h(v_h), \quad \forall v_h \in \mathcal{V}^h, \\ & C_h(\alpha_h, u_h) \leq 0, \end{aligned} \tag{4.4}$$

where J_h and C_h are the discrete version of the objective and constraint functions, and the space of admissible designs, $\mathcal{U}_h$ is the set of element-wise constant functions. There are different optimization methods to solve the optimization problem (4.4), for instance, the optimality criteria method [30] and the Method of Moving Asymptotes (MMA) [31]. The MMA method is well suited mathematical algorithm for topology optimization problems [29]. We use the MMA to solve the topology optimization problem in Paper B.

4.3 Penalization

Unfortunately, the relaxed problem (4.2) is different from the original binary problem (4.1), and the material indicator function corresponding to the relaxed problem is usually not binary. This results in "gray" regions in the optimized designs. However, the goal of the original problem is to find a black and white structure, that is, a solution α such that $\alpha(x)$ is either ε or 1 for all points $x \in \Omega$. To obtain binary optimal designs, it is common to introduce some kind of penalization to force the intermediate values towards either ε or 1.

There are different penalization methods in topology optimization. One of the methods, commonly used in acoustic related problems, deals with the intermediate values by adding a penalty function J_p to the objective function (4.2a), and optimizes the penalized problem

$$\min_{\alpha \in \mathcal{U}} J(\alpha, u) + \gamma J_p(\alpha) \tag{4.5a}$$

$$\text{s.t. } a(\alpha; u, v) = \ell(v), \quad \forall v \in \mathcal{V}, \tag{4.5b}$$

$$C(\alpha, u) \leq 0. \tag{4.5c}$$

Alternatively, the penalty function can be added as a constraint by including

$$J_p(\alpha) \leq \varepsilon_p,$$

in the problem (4.2), for a small positive number ε_p. One of the frequently used penalty functions [32, 33], is

$$J_p(\alpha) = \int_\Omega (1-\alpha)(\alpha - \varepsilon). \tag{4.6}$$

For topology optimization problems with *active* volume constraint, the so called Solid Isotropic Material with Penalization (SIMP) method is widely used. It was suggested by Bendsøe [34] and uses a non-linear interpolation function of the form

$$f_q(\alpha) = \alpha^q, \tag{4.7}$$

where $q > 1$ is a constant, together with the volume constraint

$$\int_\Omega \alpha(x)dx \leq V. \tag{4.8}$$

In this method, as the value of q increases the local stiffness of the intermediate values decreases while their volume are unchanged. An alternating approach to the SIMP method is RAMP (Rational Approximation of Material Properties)

$$f_q(\alpha) = \frac{\alpha}{1+q(1-\alpha)}, \tag{4.9}$$

with $q > 0$, which was introduced by Rietz [35] and analyzed by Stolpe and Svanberg [36]. In these cases, the parameter q represents the amount of penalization, and the variational equation in problem (4.2) is replaced by

$$a(f_q(\alpha); u, v) = \ell(v), \quad \forall v \in \mathcal{V},$$

with volume constraint (4.8).

4.4 Numerical instabilities and regularization

A well-organized survey of numerical instabilities in topology optimization for continuum elastic structures and their corresponding regularization methods is given by Sigmund and Petersson [28]. In this section, a brief overview of numerical instabilities and a possible treatment method is presented. In general the common numerical problems arising in topology optimization can be categorized in to three groups: *mesh dependency*, formation of *checkerboard pattern*, and *local minima*.

Mesh dependency is the problem of finding qualitatively different solutions with more and more holes and finer structural elements with better results when the problem is solved using the same algorithm but with finer and finer mesh sizes. It is related

to the non-existence of solution to the optimization problem, due to non-closedness of the set of feasible designs.

A checkerboard pattern is the occurrence of high oscillations of the design variable between air and material. The issue is usually associated with the choice of finite elements and can often be prevented by using higher-order finite element for the state variable [37].

Most problems in topology optimization are not convex and many of them have multiple (local) minima [29]. Hence, performing the same numerical optimization algorithm but with a small change in the starting guess or algorithmic parameters can result different locally optimal solutions. Based on experience, a continuation approach is suggested to overcome this problem [28, 29]. This approach lets the penalization parameters increase or decrease gradually in order to guide the development of the solution towards reliably good designs.

In the literature, several methods are proposed to tackle the problems with checkerboard patterns and mesh-dependency in topology optimization [28, 29, 34]. Mesh-independent filtering methods are among the most common such methods due to their ease of implementation and their efficiency [38]. The use of filtering in topology optimization, based on ideas borrowed from image processing, was suggested by Sigmund [39]. Since then, filters have been used in order to regularize many topology optimization problems [33, 40, 41, 42]. Filtering methods engaged to regularize topology optimization problems can be grouped into *density* and *sensitivity* based methods.

Density filtering was introduced by Bruns and Tortorelli [40]. The main idea is to modify the element density such that it depends on the densities of elements in a predefined neighborhood. The problem is optimized with respect to an artificial density variable $\widehat{\alpha}$ and the physical density, the filtered one, is achieved by using a convolution of a filter kernel and the artificial density variable, given by

$$\alpha(x) = \int_{\mathbb{R}^d} \phi(x, y)\widehat{\alpha}(y)dy, \tag{4.10}$$

where d is the space dimenstion. The filer kernel ϕ, typical in topology optimization, is

$$\phi(x, y) = \sigma(x) \max\left(0, 1 - \frac{|x - y|}{\tau}\right), \tag{4.11}$$

where $\tau > 0$ is the filter radius and $\sigma(x)$ is a normalization factor such that

$$\int_{\mathbb{R}^d} \phi(x, y)dy = 1.$$

Bourdin [41] proved the existence as well as finite element convergence of the minimum compliance problem using this filter and the SIMP penalization method. In Paper B, we use density filtering with an anisotropic generalization of integration kernel (4.11). The filtered and penalized version of the topology optimization

problem (4.2) is given by

$$\begin{aligned} &\min_{\widehat{\alpha}\in\mathcal{U}} J(\alpha,u)+\gamma J_p(\alpha) \\ &\text{s.t. } \alpha(\cdot)=\int_{\mathbb{R}^d}\phi(\cdot,y)\widehat{\alpha}(y)dy \\ &\qquad a(\alpha;u,v)=\ell(v), \quad \forall v\in\mathcal{V}, \\ &\qquad C(\alpha,u)\leq 0. \end{aligned} \tag{4.12}$$

The other alternative, sensitivity filtering, is used to modify the design sensitivity of a particular element by making it dependent on a weighted average over its neighboring elements. In this method, the design updates are performed using the filtered sensitivity instead of the real sensitivity. It is a simple approach to use but risky too, especially for line-search based optimization algorithms [38]. Different variations of the two filtering methods are reviewed in Sigmund's article [38]. Alternative techniques that could be used to produce black and white solutions are presented in the survey article [28] by Sigmund and Petersson.

Chapter 5

Summary of Paper B - Anisotropic Topology Optimization of a Reactive Muffler with a Perforated Pipe

5.1 Introduction

In Paper B, we consider the optimal design of a reactive muffler. A reactive muffler is a device commonly used to attenuate exhaust noise of internal combustion engines. It consists of a series of chambers of different dimensions connected together to cause impedance mismatch, that is, to reflect a substantial part of the acoustic energy back to the source or back and forth among the chambers [43]. Any change on the arrangement or dimensions of the muffler components affect the performance.

We used topology optimization by material distribution to optimize the internal configuration of an expansion chamber in a cylindrical symmetric reactive muffler. The objective is to reduce the outgoing acoustic energy at the outlet as much as possible by distributing sound hard material inside the expansion chamber to reflect some part of the acoustic energy back to the source. The propagation of acoustic waves in the muffler is modeled by the Helmholtz equation, and a finite element method is used to discretize the equation. The Method of Moving Asymptotes, MMA [31] is used to solve the topology optimization problem.

5.2 Problem description

We consider a muffler consisting of an expansion chamber, an end inlet and, an end outlet as shown in Figure 5.1(a). There may be a perforated pipe connecting the inlet and the outlet. The computational domain $\Omega = \Omega^{\mathrm{l}} \cup \Omega^{\mathrm{u}}$ with $\Omega^{\mathrm{u}} = \Omega^{\mathrm{d}} \cup \Omega^{\mathrm{p}}$ is illustrated in Figure 5.1(b), which is an arbitrary cross-section through the center of the cylindrical symmetric muffler 5.1(a). The non-overlapping regions Ω^{l} and Ω^{u} separated by the interface Γ_{I}. The non-design region Ω^{l} is introduced to ensure

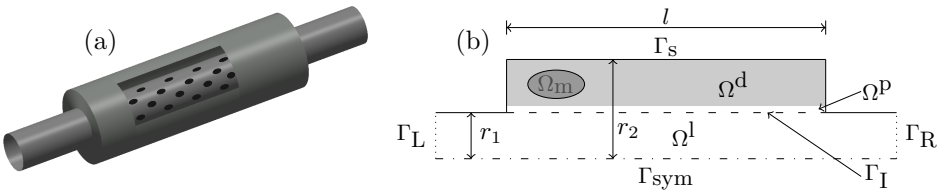

Figure 5.1: A cylindrical symmetric muffler and the computational domain.

unblocked gas flow from the inlet to the outlet. The optimization problem is to find an optimal distribution of sound-hard material in the gray-shaded design region Ω^{d} to improve the performance of the muffler. The region Ω^{m} in Figure 5.1(b) represents the region occupied by sound-hard material. The presence of material at each point in the design region is modeled by the material indicator function α, defined by $\alpha(x) = \varepsilon$ if $x \in \Omega^{\mathrm{m}}$ and $\alpha(x) = 1$ otherwise, where ε is a small positive number.

We ignore viscous losses, background flow, and hot gas effects in Ω_{a}. The inlet and outlet pipes are assumed to be narrow and long so that all non-planar modes of outgoing waves are geometrically evanescent and negligible at Γ_{L} and Γ_{R}. By assuming that the orifice diameter and the thickness of the perforated layer Γ_{I} are smaller than the wavelengths of interest, the sound propagation through the layer is modeled by an acoustic impedance.

Assume that the incoming wave at the inlet boundary, Γ_{L} is a plane wave of amplitude A. The Helmholtz equation, the boundary conditions, and the interface condition together results in the following variational problem:

$$
\begin{aligned}
&\text{Find } p^l \in H^1(\Omega^{\mathrm{l}}),\ p^u \in H^1(\Omega^{\mathrm{u}}) \text{ and } \lambda \in H^{-1/2}(\Gamma_{\mathrm{I}}) \text{ such that} \\
&\begin{cases}
\displaystyle\int_{\Omega^{\mathrm{l}}} r\nabla q^l \cdot \nabla p^l + \int_{\Omega^{\mathrm{u}}} \alpha r \nabla q^u \cdot \nabla p^u - \kappa^2 \int_{\Omega^{\mathrm{l}}} r q^l p^l \\
\quad -\kappa^2 \displaystyle\int_{\Omega^{\mathrm{u}}} \alpha r q^u p^u - \int_{\Gamma_{\mathrm{I}}} r[\![q]\!]\lambda + i\kappa \int_{\Gamma_{\mathrm{L}}\cup\Gamma_{\mathrm{R}}} r q^l p^l = 2i\kappa A \displaystyle\int_{\Gamma_{\mathrm{L}}} r q^l, \\
\qquad\qquad\qquad\qquad \displaystyle\int_{\Gamma_{\mathrm{I}}} r\mu[\![p]\!] - \frac{i}{\kappa}\int_{\Gamma_{\mathrm{I}}} r\zeta\mu\lambda = 0,
\end{cases} \\
&\text{for all } q^l \in H^1(\Omega^{\mathrm{l}}),\ q^u \in H^1(\Omega^{\mathrm{u}}), \text{ and } \mu \in H^{-1/2}(\Gamma_{\mathrm{I}}),
\end{aligned}
\tag{5.1}
$$

where r is the radial coordinate, ζ is the acoustic impedance of the perforated layer, $\kappa = \omega/c$ is the wavenumber, and $i^2 = -1$. Functions $p = p^l$ and $p = p^u$ are the complex amplitude of the pressure field in Ω^{l} and Ω^{u}, respectively, and $[\![p]\!] = p^l - p^u$.

In order to use a gradient-based optimization algorithm the binary constraint $\alpha \in \{\varepsilon, 1\}$ is relaxed into a box constraint $\alpha \in [\varepsilon, 1]$, and the optimization problem is formulated as a minimization of the transmission of acoustic energy to the muffler outlet for the target frequencies. That is,

$$\min_{\widehat{\alpha}\in\mathcal{U}} \mathcal{J}(\widehat{\alpha};\mathcal{W},\gamma), \tag{5.2}$$

where $\widehat{\alpha} \in \mathcal{U} = \{\beta \in L^\infty(\Omega) : 0 < \varepsilon \leq \beta \leq 1 \text{ a.e. in } \Omega^{\mathrm{d}}, \beta \equiv 1 \in \Omega - \Omega^{\mathrm{d}}\}$ is a new design variable, $\alpha = S(\widehat{\alpha})$ for filtering function $S : L^2(\mathbb{R}^2) \to L^2(\mathbb{R}^2)$, and $\mathcal{W}$ is the set of all frequencies for which we are interested in to optimize the muffler. The objective function is defined by

$$\mathcal{J}(\widehat{\alpha};\mathcal{W},\gamma) = J_p(S(\widehat{\alpha});\gamma) + J_t(S(\widehat{\alpha});\mathcal{W}). \tag{5.3}$$

Here, J_p is the penalty function and the *primary* objective function J_t is defined by

$$J_t(\alpha;\mathcal{W}) = \sum_{f_j\in\mathcal{W}} J(p^l(\alpha,f_j)),$$

where for each $f_j \in \mathcal{W}$, $p^l(\alpha,f_j) \in H^1(\Omega^l)$ is part of the triplet p^l, p^u, and λ that solves the state equation (5.1) for design α and wave number $\kappa = 2\pi f_j/c$ and

$$J(p^l(\alpha,f_j)) = \frac{1}{2}|\langle p^l\rangle_{\Gamma_{\mathrm{R}}}|^2,$$

where

$$\langle p^l\rangle_{\Gamma_{\mathrm{R}}} = \frac{\int_{\Gamma_{\mathrm{R}}} r p^l}{\int_{\Gamma_{\mathrm{R}}} r}.$$

The finite element method is used to discretize problem (5.1). The material indicator function is assumed to be constant in each element. The optimization problem (5.3) is solved numerically using the Method of Moving Asymptotes by adding the penalty term to the objective function using a continuation approach for the penalty parameter γ. Post-processing techniques are used in order to sharpen the edges of the sound-hard material. To compare the performance of the muffler designs, the transmission loss is used. The transmission loss of a muffler with the same cross-sectional area for the inlet and outlet is given by [44, 45]

$$TL = 10\log_{10}\left(\frac{|p_i|^2}{|p_o|^2}\right),$$

where p_i and p_o are the amplitudes of the incoming and outgoing acoustic pressure, respectively.

5.3 Selected numerical results

Two types of reactive mufflers are considered for the optimization, with and without a perforated pipe connecting the inlet and the outlet. We denote them by *muffler with impedance layer* and *muffler without impedance layer*, respectively. The mufflers have the same configuration; they have inlet and outlet pipes of radius $r_1 = 0.05$ m, and

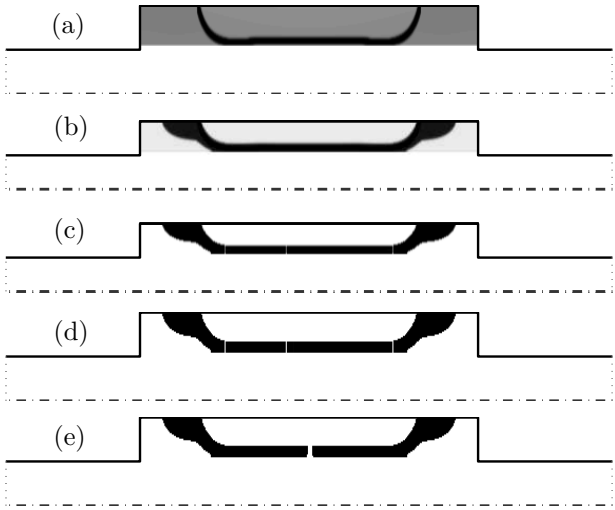

Figure 5.2: Final muffler designs from the continuation steps. (a) without penalty, (b) with penalty ($\gamma = 1/2$) and filter, (c) with penalty ($\gamma = 500$) and filter, (d) with penalty ($\gamma = 500$) and after filter is dropped, (e) after second level post-processing.

the expansion chamber has radius $r_2 = 0.1$ m and length $l = 0.5$ m. The perforated pipe of the muffler with impedance layer is characterized by a porosity of $\sigma = 20\%$, thickness $t = 1.5$ mm, and orifice diameter $d = 3.1$ mm.

For all numerical experiments, we set $\epsilon = 10^{-8}$ as a lower bound for the design variable $\widehat{\alpha}_h$. We use 28,672 square elements with side length 1.5625 mm for the finite element discretization. The number of design variables is 9,280. A plane wave of amplitude $A = 1$ is injected into the muffler at the inlet boundary.

Figure 5.2 shows the designs from different steps of the continuation approach. The optimization is performed for a muffler without impedance layer at target frequency $f = 349$ Hz. Figures 5.2(a), 5.2(b), and 5.2(c) are the designs obtained from the optimization with $\gamma = 0$, $\gamma = 1/2$ and $\gamma = 500$, respectively. It shows that as the γ increases more and more the designs become more black and white. Figure 5.2(c) looks black and white except at the edges of the sound-hard material. To obtain a sharp design, the filter is dropped and optimization is continued. Figure 5.2(d) shows the sharpened design. In this experiment, we add the second phase of post-processing, in which the three narrow openings in Figure 5.2(d) are replaced by a single opening of the same total width and the optimization is continued one more round. Figure 5.2(e) shows the final design.

We optimize the two types of mufflers for single target frequency and multi-target frequencies. The single frequency optimization is performed for a frequency of 697 Hz.

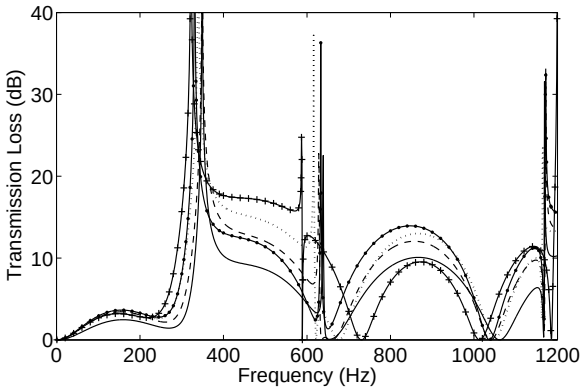

Figure 5.3: Transmission loss spectra corresponding to the designs in Figure 5.2. — TL of (a), – – TL of (b), ··· TL of (c), –●– TL of (d), –|– TL of (e).

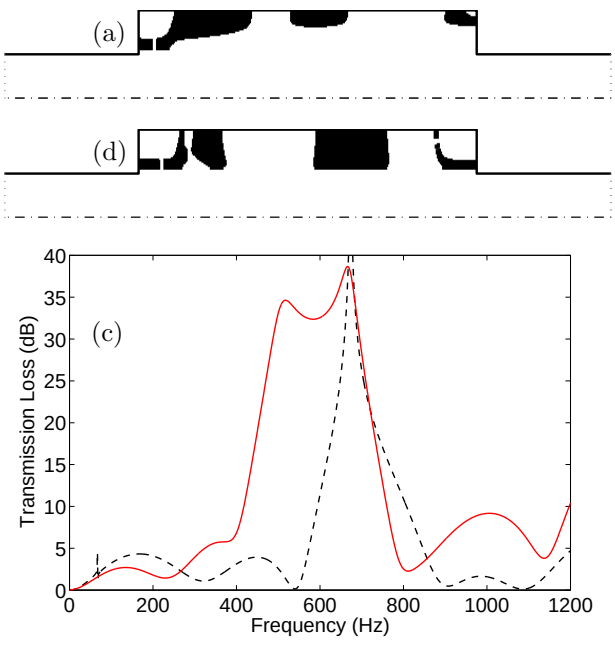

Figure 5.4: Final muffler designs and their transmission loss spectra, optimized for the target frequency 697 Hz.

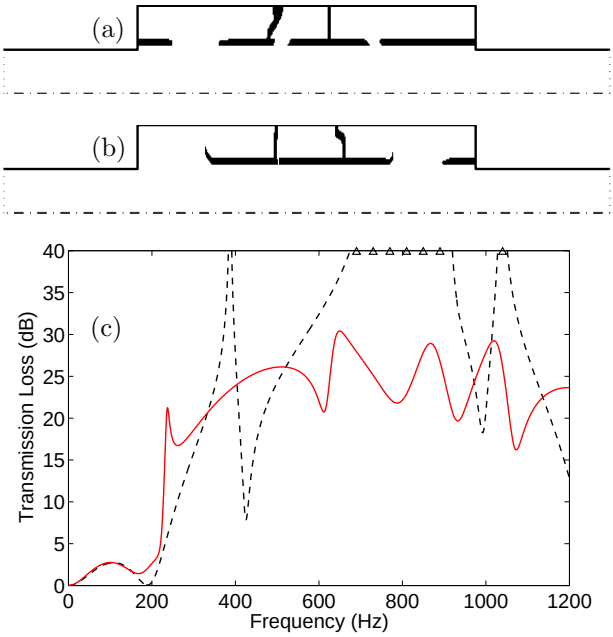

Figure 5.5: Final muffler designs and their transmission loss spectra, optimized for 20 target frequency in the range 250 – 1050 Hz.

Figures 5.4(a) and 5.4(b) show the optimized design of the mufflers without and with impedance layer, respectively and Figure 5.4(c) illustrates the transmission loss spectra of these two mufflers. The dashed line spectrum in Figure 5.4(c) shows that the design in Figure 5.4(a) performs remarkably good in the range 600 – 800 Hz. Similarly, the solid line spectrum shows that the design in Figure 5.4(b) has a good acoustic attenuation performance in the range 400 – 780 Hz.

To obtain a good performance in a wider range of frequencies we optimize for 20 frequencies exponentially distributed in the range of 250 – 1050 Hz. The optimized layout of the mufflers without and with impedance layer are depicted in Figures 5.5(a) and 5.5(b), respectively. The corresponding transmission loss spectra are illustrated in Figure 5.5(c). The spectra show that the two mufflers perform remarkably good in a range 220 – 1200 Hz.

Bibliography

[1] A. E. Bryson Jr. Optimal control—1950 to 1985. *Control Systems, IEEE*, 16(3):26–33, 1996.

[2] R. W. H. Sargent. Optimal control. *Journal of Computational and Applied Mathematics*, 124(1-2):361–371, 2000.

[3] J. T. Betts. Survey of numerical methods for trajectory optimization. *Journal of Guidance, Control, and Dynamics*, 21(2):193–207, 1998.

[4] A. E. Bryson Jr. and Y.C. Ho. *Applied Optimal Control: Optimization, Estimation, and Control*. Halsted Press book. Hemisphere Publishing Company, 1975.

[5] M. R. Hestenes. *Calculus of variations and optimal control theory*. Applied mathematics series. R. E. Krieger Pub. Co., 1980.

[6] A. E. Bryson Jr. *Applied Linear Optimal Control: Examples and Algorithms*. Cambridge University Press, 2002.

[7] D. G. Hull. *Optimal Control Theory for Applications*. Mechanical Engineering Series. Springer, 2003.

[8] L. S. Pontryagin, V. G. Boltyanskii, R. V. Gamkrelidze, and E. F. Mishchenko. *The mathematical theory of optimal processes*. Wiley, 1962.

[9] D. Burghes and A. Graham. *Control and Optimal Control: Theories with Applications*. Engineering science. Horwood Publishing Limited, 2004.

[10] D. E. Kirk. *Optimal Control Theory: An Introduction*. Dover books on engineering. Dover Publications, Incorporated, 2004.

[11] O. von Stryk and R. Bulirsch. Direct and indirect methods for trajectory optimization. *Annals of Operations Research*, 37:357–373, 1992.

[12] A. V. Rao. A survey of numerical methods for optimal control. In *2009 AAS/AIAA Astrodynamics Specialist Conference*, pages 1–37, 2009.

[13] R. Bulirsch, E. Nerz, H. J. Pesch, and O. von Stryk. Combining direct and indirect methods in optimal control: Range maximization of a hang glider. In *Optimal Control, volume 111 of International Series of Numerical Mathematics. Birkhuser*, pages 273–288. Birkhauser Verlag, 1991.

[14] T. Binder, L. Blank, H. G. Bock, R. Bulirsch, W. Dahmen, M. Diehl, T. Kronseder, W. Marquardt, J. P. Schlöder, and O. von Stryk. Introduction to model based optimization of chemical processes on moving horizons. In *Online Optimization of Large Scale Systems*, pages 295–339. Springer Berlin Heidelberg, 2001.

[15] E. Hairer, S. P. Nørsett, and G. Wanner. *Solving Ordinary Differential Equations I: Nonstiff problems*. Springer series in computational mathematics. Springer-Verlag, 1991.

[16] J. C. Butcher. *Numerical Methods for Ordinary Differential Equations*. Wiley, 2008.

[17] R. Pytlak. *Numerical Methods for Optimal Control Problems with State Constraints*. Lecture Notes in Mathematics, 1707. Springer, 1999.

[18] S. Katsumata, S. Ichinose, T. Shoji, S. Nakaura, and M. Sampei. Throwing motion control based on output zeroing utilizing 2-link underactuated arm. In *Proceedings of the 2009 conference on American Control Conference*, pages 3057–3064, 2009.

[19] U. Mettin, A. S. Shiriaev, L. B. Freidovich, and M. Sampei. Optimal ball pitching with an underactuated model of a human arm. In *IEEE International Conference on Robotics and Automation, ICRA 2010*, pages 5009–5014, 2010.

[20] M. P. Bendsøe and N. Kikuchi. Generating optimal topologies in structural design using a homogenization method. *Computer Methods in Applied Mechanics and Engineering*, 71(2):197–224, 1988.

[21] O. Sigmund. Tailoring materials with prescribed elastic properties. *Mechanics of Materials*, 20(4):351–368, 1995.

[22] S. Zhou and Q. Li. Design of graded two-phase microstructures for tailored elasticity gradients. *Journal of Materials Science*, 43:5157–5167, 2008.

[23] K. E. Jensen, P. Szabo, and F. Okkels. Topology optimization of viscoelastic rectifiers. *Applied Physics Letters*, 100(23):234102–234102–3, 2012.

[24] T. Borrvall and J. Petersson. Large-scale topology optimization in 3d using parallel computing. *Computer Methods in Applied Mechanics and Engineering*, 190(46-47):6201–6229, 2001.

[25] H. Guan, Y. J. Chen, Y. C. Loo, Y. M. Xie, and G. P. Steven. Bridge topology optimization with stress, displacement and frequency constraints. *Computers and Structures*, 81(3):131–145, 2003.

[26] L. Wang, P. K. Basu, and J. P. Leiva. Automobile body reinforcement by finite element optimization. *Finite Elem. Anal. Des.*, 40(8):879–893, 2004.

[27] L. Krog, A. Tucker, M. Kemp, and R. Boyd. Topology optimization of aircraft wing box ribs. In *10th AIAA/ISSMO Multidisciplinary Analysis and Optimization Conference*, page 16, 2004.

[28] O. Sigmund and J. Petersson. Numerical instabilities in topology optimization: A survey on procedures dealing with checkerboards, mesh-dependencies and local minima. *Structural Optimization*, 16:68–75, 1998.

[29] M. P. Bendsøe and O. Sigmund. *Topology optimization. Theory, methods, and applications*. Springer, 2003.

[30] O. Sigmund. A 99 line topology optimization code written in matlab. *Structural and Multidisciplinary Optimization*, 21(2):120–127, 2001.

[31] K. Svanberg. The method of moving asymptotes–a new method for structural optimization. *International Journal for Numerical Methods in Engineering*, 24(2):359–373, 1987.

[32] C. S. Jog and R. B. Haber. Stability of finite element models for distributed-parameter optimization and topology design. *Computer Methods in Applied Mechanics and Engineering*, 130(34):203–226, 1996.

[33] T. Borrvall and J. Petersson. Topology optimization using regularized intermediate density control. *Computer Methods in Applied Mechanics and Engineering*, 190(37-38):4911–4928, 2001.

[34] M. P. Bendsøe. Optimal shape design as a material distribution problem. *Structural and Multidisciplinary Optimization*, 1(4):193–202, 1989.

[35] A. Rietz. Sufficiency of a finite exponent in simp (power law) methods. *Structural and Multidisciplinary Optimization*, 21(2):159–163, 2001.

[36] M. Stolpe and K. Svanberg. An alternative interpolation scheme for minimum compliance topology optimization. *Structural and Multidisciplinary Optimization*, 22(2):116–124, 2001.

[37] A. Díaz and O. Sigmund. Checkerboard patterns in layout optimization. *Structural optimization*, 10:40–45, 1995.

[38] O. Sigmund. Morphology-based black and white filters for topology optimization. *Structural and Multidisciplinary Optimization*, 33(4-5):401–424, 2007.

[39] O. Sigmund. *Design of Material Structures Using Topology Optimization.* PhD thesis. Technical University of Denmark, 1994.

[40] T. E. Bruns and D. A. Tortorelli. Topology optimization of non-linear elastic structures and compliant mechanisms. *Computer Methods in Applied Mechanics and Engineering*, 190:3443–3459, 2001.

[41] B. Bourdin. Filters in topology optimization. *International Journal for Numerical Methods in Engineering*, 50(9):2143–2158, 2001.

[42] M. Y. Wang and S. Wang. Bilateral filtering for structural topology optimization. *International Journal for Numerical Methods in Engineering*, 63(13):1911–1938, 2005.

[43] L. Munjal. *Acoustics of ducts and mufflers with application to exhaust and ventilation system design.* Wiley-Interscience publication. Wiley, 1987.

[44] T. W. Wu and G. C. Wan. Muffler performance studies using a direct mixed–body boundary element method and a three-point method for evaluating transmission loss. *Journal of Vibration and Acoustics*, 118(3):479–484, 1996.

[45] D. D. Davis, G. M. Stokes, D. Moore, and G. L. Stevens. Theoretical and experimental investigation of mufflers with comments on engine-exhaust muffler design. NACA report 1192, 1954.